

Modulating Charge Transfer through Cyclic D,L- α -Peptide Self-Assembly

W. Seth Horne, Nurit Ashkenasy, and M. Reza Ghadiri*^[a]

Abstract: We describe a concise, solid support-based synthetic method for the preparation of cyclic D,L- α -peptides bearing 1,4,5,8-naphthalenetetracarboxylic acid diimide (NDI) side chains. Studies of the structural and photoluminescence properties of these molecules in solution show that the hydrogen bond-directed self-assembly of the cyclic D,L- α -peptide backbone pro-

motes intermolecular NDI excimer formation. The efficiency of NDI charge transfer in the resulting supramolecular assemblies is shown to depend on the length of the linker between the NDI

and the peptide backbone, the distal NDI substituent, and the number of NDIs incorporated in a given structure. The design rationale and synthetic strategies described here should provide a basic blueprint for a series of self-assembling cyclic D,L- α -peptide nanotubes with interesting optical and electronic properties.

Keywords: charge transfer • cyclic peptides • nanotubes • self-assembly • supramolecular chemistry

Introduction

Cyclic D,L- α -peptides are the archetypical members of a growing class of organic tubular supramolecular structures^[1–8] with promising potential applications in biological^[9] and materials^[10] settings. As a result of increasing interest in the field of molecular electronics,^[11] theoretical calculations have been used to assess the conductive properties of self-assembling peptide nanotubes.^[12] It has been proposed that the cyclic D,L- α -peptide structures should possess wide band gaps ($E_g > 4$ eV) that could potentially be tuned through appropriate modification of the cyclic peptide.^[12a] However, it has been determined that natural amino acid side chains cannot be used to decrease the band gap to levels sufficient for potential use in molecular electronics applications. Since many organic semiconducting and conducting materials are based on one-dimensional stacking of aromatic molecules through π - π interactions and partial charge transfer,^[13] we envisioned that cyclic peptide self-assembly might be useful in controlling and directing the stacking of aromatic side

chains and might offer a level of control over the long-range order in the resulting materials.^[1,10b,14]

Among aromatic molecules that have found utility in the design of conductive materials, naphthalenediimide derivatives have attracted considerable attention due to their tendency to form n-type materials, as opposed to most other organic molecules, used to fabricate p-type semiconductors.^[15] High-conductivity materials based on NDI-derivatized dendrimers and polymers have also been reported.^[16] We postulated that the intermolecular interactions of NDIs could be directed and/or promoted by the display of such species as side chains of cyclic D,L- α -peptides. It was envisioned that controlling aromatic ring interactions and geometry through peptide backbone-directed self-assembly^[17] might provide a rational supramolecular approach to conductive materials engineering. To these ends, we present here a model system for probing hydrogen bond-directed intermolecular NDI–NDI interactions in solution. We report methods developed for the synthesis of NDI-modified cyclic D,L- α -peptides, examine their propensity for self-assembly by NMR, and probe the efficiency of intermolecular NDI–NDI charge transfer by fluorescence measurements.

Results and Discussion

Design: Cyclic D,L- α -peptides can form cylindrical β -sheet ensembles through hydrogen bond-directed ring stacking.^[2] Interruption of the hydrogen bonding network on one face of the cyclic peptide subunit through backbone N-alkylation

[a] W. S. Horne,[†] Dr. N. Ashkenasy,[†] Prof. M. R. Ghadiri
Departments of Chemistry and Molecular Biology and The Skaggs
Institute for Chemical Biology
The Scripps Research Institute
10550 North Torrey Pines Rd., La Jolla, CA 92037 (USA)
Fax: (+1) 858-784-2798
E-mail: ghadiri@scripps.edu

[[†]] These authors contributed equally to this work.

restricts the self-assembly to antiparallel cylindrical dimers (Figure 1a).^[18,19] Such assemblies represent the asymmetric unit of the parent extended peptide nanotube and have proven to be useful models for probing of the nanotube structure, self-assembly process, and functional properties.^[10a,17–20] Here we have used this strategy to investigate the design and optical properties of NDI-functionalized self-assembling cyclic *D,L*- α -peptides.

Modeling suggests that NDI-modified side chains could adopt productive charge-transfer geometries in the context of the cyclic *D,L*- α -peptide dimer (Figure 1b, c). Accordingly, peptides **1–5** were designed to probe the influence of linker length, distal NDI substituent, and number of NDI amino acid side chains on the dimer self-assembly and optical properties. Peptides **1–3**, each with a single NDI side chain, were designed to evaluate the effects of steric bulk of the distal NDI substituent (methyl in **3** versus isobutyl in **1** and **2**). The effect of linker length was examined by comparison

of the properties of cylindrical dimers derived from peptides **1** and **2**. Peptides **4** and **5**, each bearing two NDI side chain functionalities, were designed similarly in order to examine the role of multiple NDI substitutions and linker length. It should be noted that ring symmetry is an important design consideration in these molecules, as it determines the number of non-equivalent dimeric assemblies that a given cyclic peptide can form.^[17,19] In the flat ring conformation adopted by an eight-residue cyclic *D,L*- α -peptide in a nanotube context, the backbone is C_4 symmetric with the axis of rotation perpendicular to the plane of the ring.^[2b,19] Accordingly, the dimer shown in Figure 1a represents only one of four possible diastereomeric assemblies differing in the cross-strand pairing of homochiral amino acids. Depending on the peptide sequence, one or more of these dimers may be equivalent. Therefore, the C_1 symmetric peptides **1–3** can each form four different diastereomeric assemblies (Figure 1d), whereas the C_2 -symmetric eight-residue peptides **4**

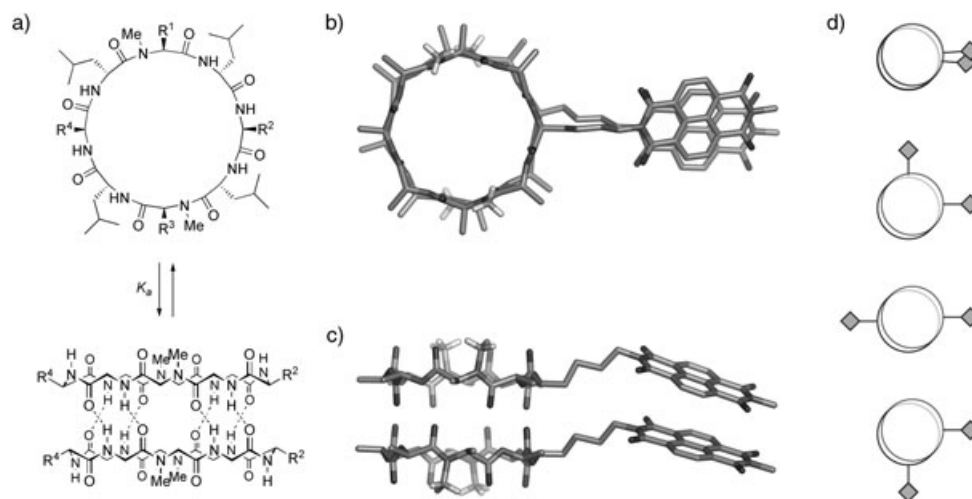
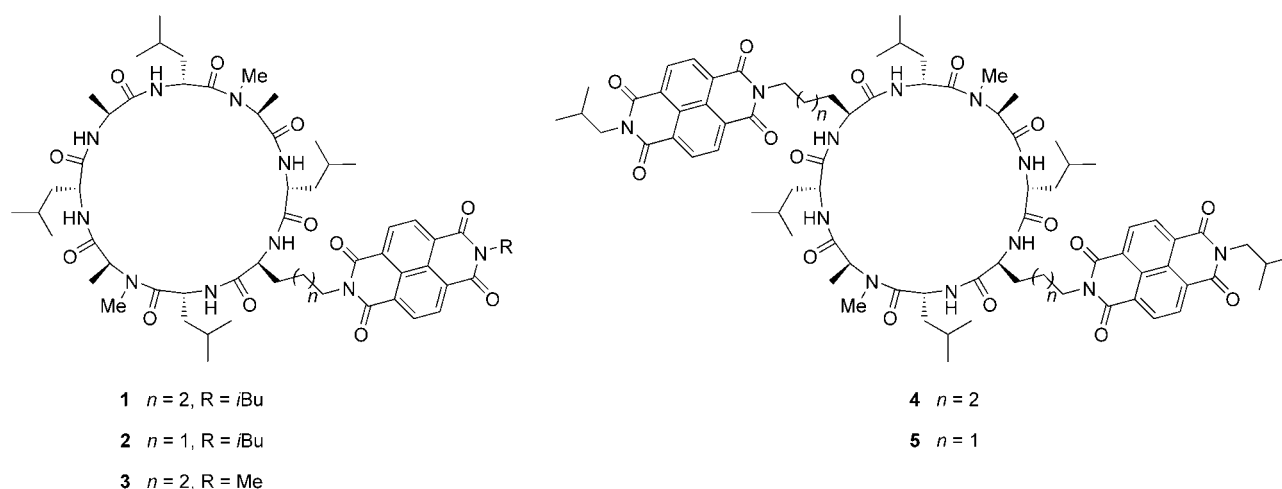
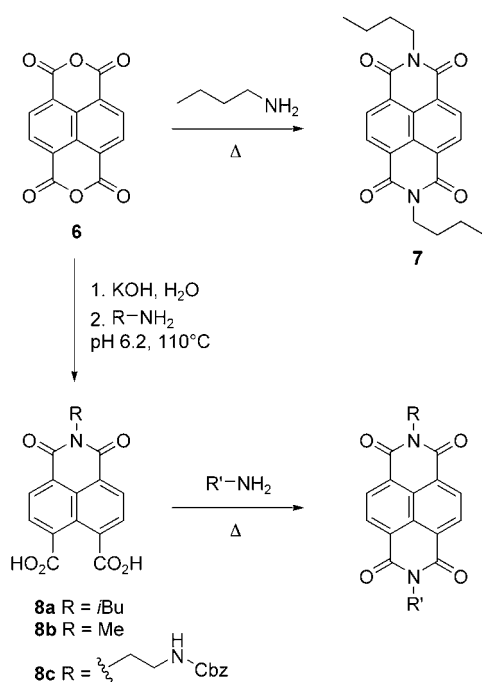


Figure 1. a) Schematic representation of hydrogen bond-directed dimerization of backbone *N*-methylated cyclic *D,L*- α -peptides with generic side chains R^1 – R^4 (for clarity most side chains are not depicted in dimeric assembly). b) Calculated model of one possible dimer of peptide **3** viewed from the top and c) from the side (most side chains and protons omitted for clarity). d) Schematic illustration depicting overlap of NDI side chains (diamonds) in the four possible dimeric assemblies available to the C_1 -symmetric peptides **1**, **2**, and **3**.



and **5** can each form a maximum of two diastereomers. This is an important consideration, as inter-subunit NDI–NDI interactions should only be possible in dimeric species in which the aromatic side chains are juxtaposed across each other on opposite rings.

Synthesis: We investigated three synthetic routes toward the desired cyclic peptides bearing NDI side chains. These routes included preparation from an NDI-functionalized amino acid,^[21] post-synthetic modification^[16c] of cyclic D,L- α -peptides, and modification of natural amino acid side chains during the course of solid-phase peptide synthesis.^[22] For the synthesis of peptides **1–5** we found the last approach to be most general and synthetically convenient. Central to each of these approaches is the preparation of unsymmetrically substituted NDIs. Symmetrical NDIs such as *N,N'*-dibutyl-1,4,5,8-naphthalenetetracarboxylic acid diimide (**7**) can be prepared by condensation of 1,4,5,8-naphthalenetetracarboxylic acid dianhydride (**6**) with two equivalents of a primary amine (Scheme 1).^[23] Unsymmetrical NDIs present a

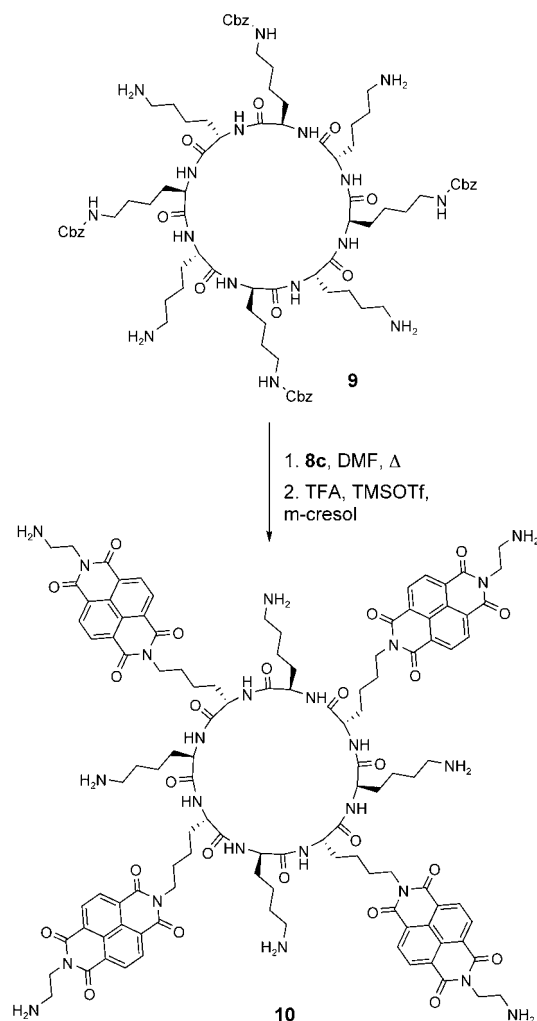


Scheme 1. Preparation of symmetrical and unsymmetrical NDI derivatives.

greater challenge and have typically been prepared from anhydride **6** by condensation with 1:1 mixtures of two different primary amines, leading to statistical mixtures of products. We have found a modification of a reported synthesis of NDI cyclophanes^[24] to be a convenient alternative to this approach (Scheme 1). After complete hydrolysis of a suspension of **6** (20 mM in water) with KOH, reacidification to pH 6.2 with H_3PO_4 leads to the formation of the diacid naphthalenetetracarboxylic acid monoanhydride. Addition

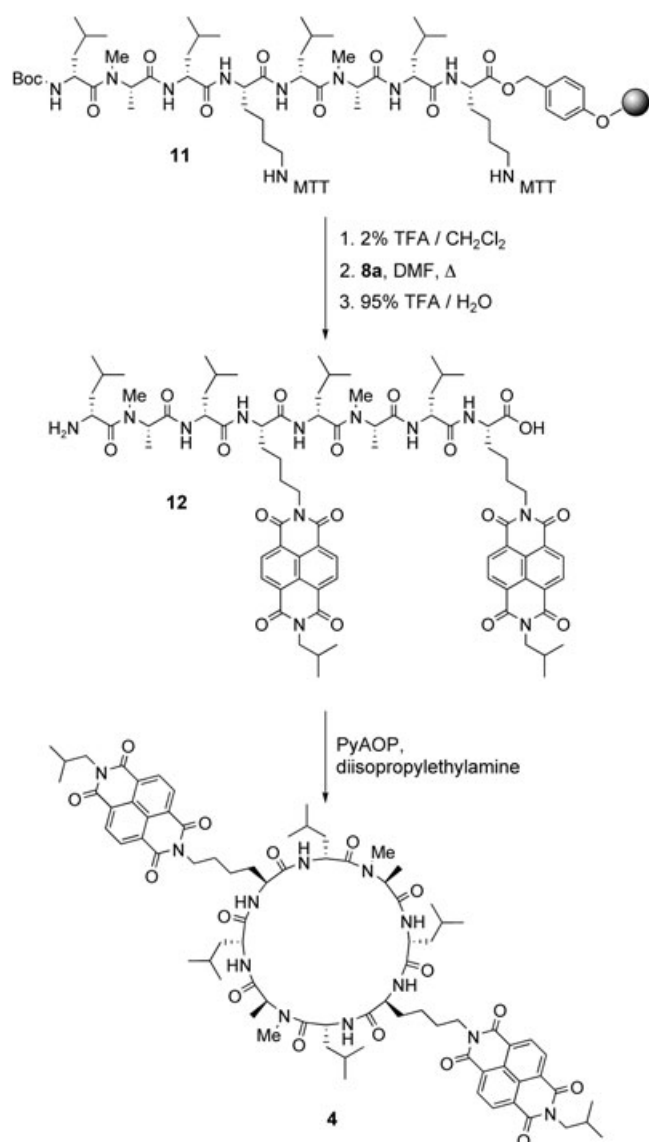
of one equivalent of a primary amine to the same reaction vessel, followed by overnight heating at reflux, yields naphthalene monoimides **8a–c** in good isolated yield and purity by a simple filtration workup.

We found that the dicarboxylic acid moieties in **8a–c** could be directly converted into imides by condensation with primary amines in DMF at temperatures above 110°C without the need to isolate the corresponding anhydrides first.^[16c,24] In one example of the use of monoimides (**8**) in the synthesis of cyclic D,L- α -peptides (Scheme 2), the four



Scheme 2. Use of naphthalene monoimides in the post-synthetic modification of cyclic D,L- α -peptides.

free amine lysine side chains of peptide **9** were converted into diimides by heating at 115°C with Cbz-ethylenediamine-modified monoimide **8c** in DMF. Removal of the Cbz protecting groups and purification yielded tetra-NDI-substituted peptide **10** in 38% overall yield for the two steps. Naphthalene monoimides were also incorporated onto peptides by on-resin conversion of lysine or ornithine side chain



Scheme 3. On-resin conversion of side chain amines into imides.

amines into imides (Scheme 3). A representative synthesis began with the preparation of linear peptide **11** by standard Fmoc solid-phase peptide synthesis methods, with use of MTT-protected (MTT = ϵ -4-methyltrityl) lysine. Resin-bound **11** was treated with dilute TFA to remove the MTT protecting groups, and the resulting free amines were converted into imides by stirring the resin with an excess of **8b** in DMF at 110°C. The NDI-modified linear peptide was cleaved from the resin by treatment with TFA and purified by preparative HPLC to yield **12** in 28% overall yield. Treatment of **12** with (7-azabenzotriazol-1-yloxy) tripyrrolidinophosphonium hexafluorophosphate (PyAOP) and diisopropylethylamine at 0.7 mM in DMF led to formation of the desired cyclic product **4** in 71% isolated yield. This synthetic approach was also used to prepare peptides **1**, **2**, **3**, and **5**.

NMR structural characterization: NMR was utilized to probe the three-dimensional structures and assembly of peptides **1–5** in CDCl₃. The ¹H NMR spectra at low concentrations ($\approx 200 \mu\text{M}$) are sharp and consistent with the preponderance of monomeric species in solution. The spectra of peptides **4** and **5** show peaks for only four different residues, indicating that these peptides maintain an apparent C₂ symmetry in solution. For each peptide, an increase in concentration leads to a new set of peaks consistent with hydrogen-bonded dimeric species in slow exchange (on the NMR timescale) with the monomer.^[19a] The concentration-dependent monomer/dimer ratio was used to determine the apparent self-association constants (K_a values) (Table 1). In

Table 1. Association constants as determined by NMR spectroscopy.

Cpd	Sequence ^[a]	K_a ^[b] [M ⁻¹]
1	<i>cyclo</i> [Ala-Leu ^{Me} Ala-Leu-Lys _{NDI-iBu} -Leu ^{Me} Ala-Leu]	116
2	<i>cyclo</i> [Ala-Leu ^{Me} Ala-Leu-Orn _{NDI-iBu} -Leu ^{Me} Ala-Leu]	192
3	<i>cyclo</i> [Ala-Leu ^{Me} Ala-Leu-Lys _{NDI-Me} -Leu ^{Me} Ala-Leu]	119
4	<i>cyclo</i> [(Lys _{NDI-iBu} -Leu ^{Me} Ala-Leu) ₂]	52
5	<i>cyclo</i> [(Orn _{NDI-iBu} -Leu ^{Me} Ala-Leu) ₂]	87
7	dibutyl-NDI	0.4

[a] Italic residues indicate D enantiomers; ^{Me}Ala = N-methylalanine.
[b] Details of the calculations can be found in the Experimental Section.

the calculation of the association constants, all possible diastereomeric ensembles formed by a given peptide were considered equivalent, so the K_a values in Table 1 reflect the overall propensity for self-association demonstrated by each peptide. The ¹H NMR data fit well with the self-association model, and the results of the calculations show that peptides in CDCl₃ form dimeric species with K_a values ranging from 51 to 192 M⁻¹.

Direct comparison of the association constants for the non-symmetric peptides **1–3** with those of the C₂-symmetric peptides **4** and **5** is complicated by two factors. The non-equivalent diastereomeric assemblies that can be formed through the dimerization of the peptide give rise to an entropy of mixing term that varies with the number and population of those assemblies.^[25] In addition, a free energy term arising from the symmetry difference between the peptide monomer and dimer contributes a symmetry component— independent of the inherent chemical propensity to self-associate—to the observed K_a .^[26] Calculations for the C₁- and C₂-symmetric peptides, however, show that the energetic contributions from these two terms cancel if it is assumed that a statistical mixture of dimeric assemblies is formed.

The differences in the binding constants of the various molecules provide some insight into the effect of the NDI modification on assembly of the peptide backbone. Comparison of the single-NDI-containing peptides **1** and **2** with the bis-NDI peptides **4** and **5**, respectively, show a twofold decrease in the binding constants accompanying the incorporation of an additional NDI side chain. This suggests that multiple NDIs on a cyclic peptide would tend to destabilize

dimer formation. Comparison of **4** with **5** and of **1** with **2** show $\approx 60\%$ decreases in K_a for the lysine-based linkers, indicating that the dimer is more stable when the NDI group is tethered closer to the peptide backbone. The similar association constants for **1** and **3** indicate that the distal NDI substituent has little impact on intermolecular peptide self-association.

Fluorescence characterization: Charge delocalization as a consequence of aromatic ring stacking provides the basis of the electronic properties observed in high-order NDI aggregates. Charge transfer within an NDI dimer in solution leads to the formation of excimers, which can be conveniently monitored by fluorescence spectroscopy.^[27] Thus, the role of cyclic peptide backbone self-assembly in enhancing NDI–NDI interactions was probed through fluorescence measurements. Figure 2a shows the fluorescence spectra for single-

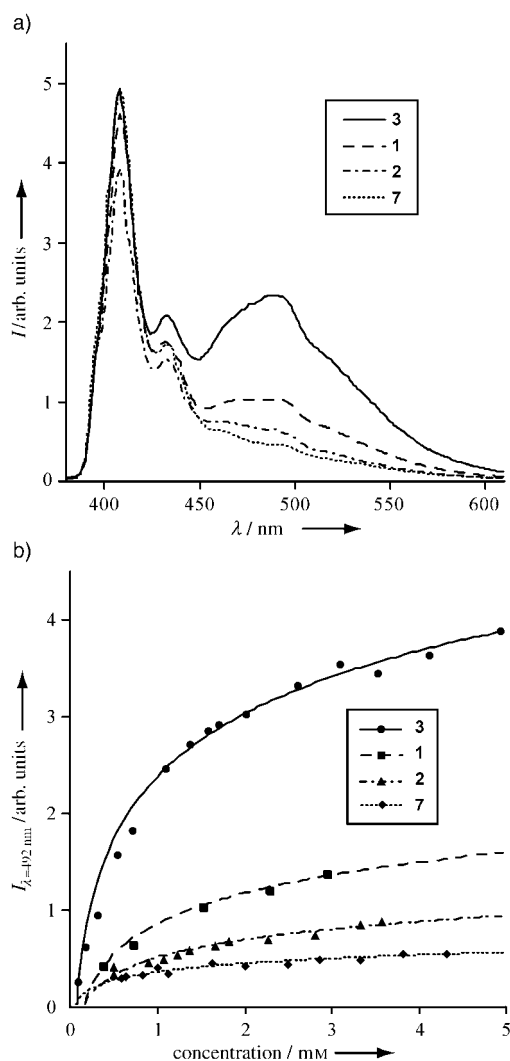


Figure 2. a) Fluorescence spectra of 1.65 mM solutions of peptides **1**, **2**, **3**, and control compound **7** in CDCl_3 ($\lambda_{\text{exc}} = 330\text{ nm}$). b) The change in excimer intensity as a function of peptide concentration (lines are shown to guide the eye).

NDI-containing peptides **1**, **2**, and **3** and also for the control compound **7** at 1.65 mM in CDCl_3 . The formation of excimers is indicated by the presence of a broad peak with a maximum at 492 nm, red-shifted with respect to the monomeric peaks at wavelengths of 434 and 408 nm due to charge delocalization. As would be expected from the peptide self-assembly observed by NMR, all three peptides (**1**–**3**) show enhanced excimer peak intensity relative to the control compound **7**. These effects can be seen throughout the concentration range (0.1–5 mM) studied (Figure 2b).

Although the practical range of peptide concentrations that can be studied (as determined by the magnitude of K_a) is above the region in which rigorous quantitative analysis of the fluorescence data is possible, some qualitative differences are clear. Differences in excimer peak intensity suggest that, in addition to the enhanced effective concentration brought about by peptide backbone-directed self-assembly, other structural parameters also seem to play a role in the formation of NDI excimers. It is evident that peptide **3** has a much higher propensity than **1** for the formation of NDI excimers. Since the NMR data show similar association constants for the two peptides, the difference in excimer formation can be attributed to the reduced steric hindrance from the distal NDI methyl group in **3** in relation to the branched isobutyl moiety in **1**, allowing more productive interactions between the aromatic rings.

The length of the tether between the peptide backbone and the NDI substituent also seems to influence NDI excimer formation. Peptide **1** shows more pronounced excimer formation than the control compound **7**, while **2**—which by NMR has an association constant almost twice that of **1**—shows excimer peak intensity closer to that of the control compound. This suggests that the shorter ornithine-based linker between the NDI and the cyclic peptide backbone in **2** does not allow the necessary flexibility for the NDI side chains on adjacent peptide strands to adopt an orientation suitable for efficient charge transfer. In contrast with the effect of linker length on peptide dimerization, the additional degrees of freedom offered by the lysine-based linker in this case allow more favorable intermolecular NDI interactions relative to the shorter ornithine.

As discussed above, in the non-symmetrically substituted peptide **3**, the dimer in which the NDI side chains are juxtaposed across from each other represents only one of four possible diastereomeric assemblies (Figure 1d). In calculation of the apparent association constants reported in Table 1, these dimers were all considered equivalent. It is reasonable to assume that only the assembly in which the NDI side chains overlap would be productive with respect to intermolecular excimer formation (Figure 1b, c). However, this dimer is probably the least stable and therefore least populated of the four, as the other three have the bulky NDI moiety paired with less sterically demanding alanine side chains. Although peptides **4** and **5** show K_a values two orders of magnitude larger than that of **7** by NMR spectroscopy, efforts to probe the efficiency of the intermolecular NDI charge transfer in these C_2 -symmetric peptides were

not informative, due to interference by intramolecular NDI interactions. The fluorescence spectrum of each exhibits a large concentration-independent excimer peak (data not shown). This peak remains even at concentrations at which the ^1H NMR indicates that only monomers exist in solution for both peptides, suggesting that there is enough flexibility in the peptide backbone to allow productive intramolecular interaction between NDI side chains. As would be expected, this intramolecular NDI excimer formation depends on linker length and is more pronounced in **4** than **5**.

In conclusion, these studies indicate that cyclic D,L- α -peptide self-assembly can be an effective process for templating directed aromatic side chain–side chain interactions. It might therefore be expected that the design rationale described here, coupled with the efficient synthetic process, should allow access to a variety of cyclic D,L- α -peptide sequences bearing NDI side chains for use in the construction of self-assembling peptide nanotube analogues with novel optical and electronic properties.

Experimental Section

General: The Fmoc-amino acids, resins used for solid-phase peptide synthesis, and 2-(1*H*-benzotriazol-1-yl)-1,1,3,3-tetramethyluronium hexafluorophosphate (HBTU) were all purchased from Novabiochem. NMR solvents were obtained from Cambridge Isotope Labs. *N*-Cbz-ethylenediamine hydrochloride was purchased from TCI America. (7-Azabenzotriazol-1-yloxy) tripyrrolidinophosphonium hexafluorophosphate (PyAOP), 1,4,5,8-naphthalenetetracarboxylic acid dianhydride (**6**), and all other solvents and reagents were purchased from Aldrich. DMF used in coupling and cyclization steps was dried over 4 Å molecular sieves. All other reagents and solvents were used as received. Reversed-phase HPLC was carried out on C_{18} columns with use of water/acetonitrile/TFA gradients between 99:1:0.1 and 10:90:0.1. NMR spectra were obtained on Bruker AMX 400, DRX 500, or DRX 600 spectrometers. UV/Vis measurements were made on a Cary 100 Bio UV/visible Spectrophotometer. Fluorescence spectra were acquired on an Aminco Bowman Series 2 Luminescence Spectrometer.

Monoimide 8a: 1,4,5,8-Naphthalenetetracarboxylic acid dianhydride (**6**, 2.0 g, 7.46 mmol) was weighed into a 500-mL flask. Water (350 mL) was added, followed by KOH (1 M, 35 mL). In some cases, heat, sonication, and/or additional KOH were used to dissolve the starting material completely. After the solid had dissolved, the solution was acidified to pH 6.4 with H_3PO_4 (1 M). Isobutylamine (0.741 mL, 7.46 mmol) was added, and the solution was again acidified to pH 6.4 with H_3PO_4 (1 M). The reaction vessel was fitted with a reflux condenser, and the mixture was heated to 110°C, stirred overnight, allowed to cool to room temperature, and filtered. Acetic acid (5 mL) was added to the filtrate, and a white solid precipitated from the solution. The solid was collected by filtration, washed with water, and dried under high vacuum to yield the desired product (1.714 g, 67%) as an off-white solid. ^1H NMR (400 MHz, $[\text{D}_6]\text{DMSO}$): δ = 8.51 (d, J = 7 Hz, 2H), 8.07 (d, J = 7 Hz, 2H), 3.90 (d, J = 7 Hz, 2H), 2.12 (m, 1H), 0.90 ppm (d, J = 7 Hz, 6H); ^{13}C NMR (100 MHz, $[\text{D}_6]\text{DMSO}$): δ = 169.7, 163.3, 130.3, 128.6, 128.1, 128.0, 125.5, 123.4, 46.6, 26.9, 20.2 ppm; MALDI-FTMS: found: 342.0972 $[M+H]^+$; calcd 342.0964.

Monoimide 8b: This compound was prepared by treatment of 1,4,5,8-naphthalenetetracarboxylic acid dianhydride (**6**, 1.0 g, 3.73 mmol) with methylamine hydrochloride (252 mg, 3.73 mmol) as described for **8a**. The reaction yielded the product (890 mg, 80%) as a pale yellow solid. ^1H NMR (500 MHz, D_2O): δ = 8.56 (d, J = 8 Hz, 2H), 8.05 (d, J = 8 Hz, 2H), 3.47 ppm (s, 3H); ^{13}C NMR (125 MHz, $\text{NaOD}/\text{D}_2\text{O}$, DSS as internal

standard): δ = 178.0, 169.1, 147.6, 134.0, 131.6, 129.5, 127.5, 124.8, 29.6 ppm; ESI-TOF MS: found: 298.0360 $[M-H]^-$; calcd 298.0357).

Monoimide 8c: This compound was prepared by treatment of 1,4,5,8-naphthalenetetracarboxylic acid dianhydride (**6**, 1.163 g, 4.34 mmol) with *N*-Cbz-ethylenediamine hydrochloride (1.0 g, 4.33 mmol) as described for **2a**. The reaction yielded the product (1.129 g, 56%) as a pale tan solid. ^1H NMR (400 MHz, $[\text{D}_6]\text{DMSO}$): δ = 8.50 (d, J = 8 Hz, 2H), 8.07 (d, J = 8 Hz, 2H), 7.4–7.2 (m, 6H), 4.94 (s, 2H), 4.16 (t, J = 6 Hz, 2H), 3.60 ppm (q, J = 6 Hz, 2H); ^{13}C NMR (150 MHz, $[\text{D}_6]\text{DMSO}$ with 4 equiv triethylamine to improve solubility): δ = 170.8, 163.6, 156.2, 146.3, 137.2, 129.9, 128.7, 128.1, 127.5, 127.4, 126.3, 125.7, 121.6, 64.9, 38.2 ppm; ESI-TOF MS (m/z) found: 461.0989 $[M-H]^-$; calcd 461.0990.

Cyclic peptide 9: Peptide **9** was prepared by the previously reported methodology from Fmoc-Lys-OAllyl attached through the amine of the lysine side chain to 2-Cl-Trt resin.^[28] The crude material was purified by preparative RP-HPLC. ESI-TOF MS (m/z) found: 1561.9134 $[M+H]^+$; calcd 1561.9141.

NDI derivatization of a peptide in solution—synthesis of 10: Peptide **9** (11 mg, 5.5 μmol assuming a salt with four molecules of trifluoroacetate per peptide) and **8c** (12.6 mg, 27.3 μmol) were suspended in DMF (5 mL). The mixture was heated to 115°C under argon and stirred overnight. The resulting solution was allowed to cool to room temperature and concentrated to dryness. The remaining solid was washed (2 \times 2 mL) with phosphate buffer (pH 8.0), the supernatant was discarded, and the solid was dried under high vacuum. The crude solid was dissolved in TFA/trimethylsilyl trifluoromethanesulfonate/cresol (10:2:2, 200 μL). After 1 h, diethyl ether (2 mL) was added, and the resulting suspension was centrifuged. The supernatant was discarded, and the solid was washed twice more with diethyl ether (2 mL). The crude peptide was purified by preparative RP-HPLC to yield the product (6.4 mg, 38% assuming a salt with eight molecules of trifluoroacetate per peptide) as an off-white solid. ^1H NMR (600 MHz, $\text{CDCl}_3/[\text{D}]\text{TFA}$, all signals were broad, probably due to aggregation; integration of amide NH at 6.93 ppm was lower than 8 due to partial exchange with TFA): δ = 8.93 (brs, 16H), 6.93 (brs, 7H), 4.91 (brs, 8H), 4.79 (brs, 8H), 4.31 (brs, 8H), 3.82 (brs, 8H), 3.37 (brs, 8H), 2.00 (brs, 32H), 1.65 ppm (brs, 16H); ESI-TOF MS (m/z): found: 1097.4841 $[M+2H]^{2+}$; calcd 1097.4840.

Representative NDI derivatization of a peptide on solid support—synthesis of 12

1. Protected linear peptide on resin: Fmoc-Lys(MTT) Wang polystyrene resin (139 mg, 0.100 mmol) was weighed into a sintered glass peptide synthesis vessel and was allowed to swell in CH_2Cl_2 for 45 min, and then in DMF for 10 min. The resin was treated with piperidine/DMF (20%, 2 \times 8 min) to remove the Fmoc group, and washed with DMF (3 \times). A solution of Fmoc-D-leucine (142 mg, 0.40 mmol), HBTU (148 mg, 0.39 mmol), and diisopropylethylamine (175 μL , 1.0 mmol) in DMF (3 mL) was allowed to prereact for 2 min and then added to the resin. The resin suspension was agitated for 30 min, drained, and washed with DMF (3 \times). This deprotection/coupling cycle was repeated to provide the full-length linear peptide **11**. Coupling reactions following *N*-methylalanine residues were performed twice to ensure complete reaction.

2. Conversion of resin-bound Lys(MTT) into Lys(NDI) and cleavage from resin: The resin bearing **11** was washed with CH_2Cl_2 (3 \times 1 min) and treated with a CH_2Cl_2 /triethylsilane/trifluoroacetic acid mixture (93:5:2; 3 \times 2 min followed by 3 \times 10 min) to remove the lysine MTT protecting groups. The resin was then washed sequentially with CH_2Cl_2 , DMF, DMF/disopropylethylamine (95:5), and again with DMF. The resin was transferred to a 20 mL vial, to which **8a** (1.5 equiv relative to resin-bound amines, 102 mg, 0.30 mmol) was added, followed by DMF (8 mL). The suspension was heated to 110°C and stirred for 6 h. The reaction mixture was allowed to cool to room temperature and filtered through a fritted syringe. The resin was washed thoroughly (5 \times DMF, 3 \times CH_2Cl_2 , 3 \times MeOH) and dried under high vacuum. The peptide was cleaved from the resin by treatment with TFA/ H_2O (95:5) for 3 h. The cleavage mixture was collected by filtration and the resin was washed twice with TFA. The filtrates were combined and concentrated under vacuum to afford an oily residue. Water was added, and the mixture was sonicated to produce a suspension of a cream-colored solid. This mixture was frozen and

lyophilized to yield crude product. Purification by preparative RP-HPLC on a C_{18} column yielded the trifluoroacetate salt of the product (46 mg, 28%) as an off-white solid. MALDI-FTMS: found: 1507.7926 $[M+H]^+$; calcd 1507.7871.

Cyclic 4: Linear peptide **12** (46 mg, 28 μ mol) was dissolved in DMF (40 mL). PyAOP (44 mg, 85 μ mol) was added, followed by diisopropylethylamine (30 μ L, 170 μ mol). The reaction mixture was stirred for 2.5 h at room temperature and concentrated under vacuum. Water/acetonitrile/TFA (1:1:0.001, 8 mL) was added, and the residue was sonicated to create a suspension. After centrifugation, the supernatant was removed. The solid was washed twice more by the same procedure. The resulting pellet was suspended in water, sonicated, and lyophilized to yield the product (30 mg, 71%) as an off-white solid. 1H NMR (600 MHz, $CDCl_3$): δ = 8.55 (s, 8H), 7.59 (d, J = 8 Hz, 2H), 6.82 (d, J = 10 Hz, 2H), 6.55 (d, J = 7 Hz, 2H), 5.25 (q, J = 7 Hz, 2H), 4.87 (dd, J = 7, 8 Hz, 2H), 4.65 (dd, J = 6, 6 Hz, 2H), 4.46 (dt, J = 4, 10 Hz, 2H), 4.10 (m, 4H), 4.00 (d, J = 7 Hz, 4H), 2.83 (s, 6H), 2.19 (m, 2H), 1.96 (m, 2H), 1.9–1.7 (m, 8H), 1.68–1.36 (m, obscured by H_2O), 1.32 (d, J = 7 Hz, 6H), 0.97–0.93 (overlapping doublets, 24H), 0.90 (d, J = 7 Hz, 6H), 0.85 ppm (d, J = 7 Hz, 6H); MALDI-FTMS: found: 1489.7760 $[M+H]^+$; calcd 1489.7766).

Linear precursor to 1: Linear peptide was synthesized from Fmoc-Ala Wang polystyrene resin (141 mg, 0.10 mmol) and purified as described above for **12** to yield the trifluoroacetate salt of the product (27 mg, 21%) as a white solid. MALDI-FTMS: found: 1145.6621 $[M+H]^+$; calcd 1145.6605.

Cyclic 1: The linear precursor (27 mg, 21.4 μ mol) was cyclized as described for **4**. The product was purified by RP-HPLC on a C_{18} column to yield the desired product (12 mg, 50%) as a white solid. 1H NMR (600 MHz, $CDCl_3$): δ = 8.75 (d, J = 2 Hz, 4H), 7.58 (d, J = 8 Hz, 1H), 7.51 (d, J = 9 Hz), 6.86 (d, J = 9 Hz, 1H), 6.80 (d, J = 10 Hz, 1H), 6.66 (d, J = 6 Hz, 1H), 6.57 (d, J = 7 Hz, 1H), 5.24 (m, 2H), 4.85 (m, 2H), 4.59 (m, 2H), 4.46 (m, 2H), 4.15 (t, J = 8 Hz, 2H), 4.06 (d, J = 7 Hz, 2H), 2.82 (overlapping s, 6H), 2.23 (m, 1H), 1.37 (d, J = 7 Hz, 3H), 1.32 (d, J = 7 Hz, 6H), 1.95–1.40 (m, obscured by H_2O), 1.0–0.8 ppm (overlapping d, 30H); MALDI-FTMS: found: 1149.6313 $[M+Na]^+$; calcd 1149.6319.

Linear precursor to 2: Linear peptide was synthesized from Fmoc-Ala Wang polystyrene resin (141 mg, 0.10 mmol) and purified as described above for **12** to yield the trifluoroacetate salt of the product (8 mg, 6%) as a white solid. MALDI-FTMS: found: 1131.6441 $[M+H]^+$; calcd 1131.6448.

Cyclic 2: The linear precursor (8 mg, 6.4 μ mol) was cyclized as described for **4**. The product was purified by RP-HPLC on a C_{18} column to yield the desired product (4.2 mg, 59%) as an off-white solid. 1H NMR (600 MHz, $CDCl_3$): δ = 8.75 (d, J = 8 Hz, 2H), 8.72 (d, J = 8 Hz, 2H), 7.61 (d, J = 7 Hz, 1H), 7.46 (d, J = 8 Hz, 1H), 6.83 (d, J = 9 Hz, 1H), 6.77 (d, J = 8 Hz, 1H), 6.66 (brs, 1H), 6.57 (brs, 1H), 5.21 (brs, 2H), 4.83 (m, 2H), 4.66 (m, 1H), 4.56 (m, 1H), 4.48 (m, 1H), 4.44 (m, 1H), 4.15 (m, 2H), 4.06 (d, J = 8 Hz, 2H), 2.28 (s, 6H), 2.0–1.2 (overlapping multiplets obscured by H_2O peak), 1.35 (d, J = 7 Hz, 3H), 1.31 (d, J = 7 Hz, 6H), 1.0–0.87 ppm (overlapping doublets, 36H); MALDI-FTMS: found: 1113.6343 $[M+H]^+$; calcd 1113.6343.

Linear precursor to 3: The linear peptide was synthesized (from monomide **8b**) on Fmoc-Ala Wang polystyrene resin (141 mg, 0.10 mmol) and purified as described above for **12** to yield the trifluoroacetate salt of the product (16 mg, 13%) as a white solid. MALDI-FTMS: found: 1103.6113 $[M+H]^+$; calcd 1103.6135.

Cyclic 3: The linear precursor (16 mg, 13.1 μ mol) was cyclized as described for **4**. The product was purified by RP-HPLC on a C_{18} column to yield the desired product (8 mg, 56%) as an off-white solid. 1H NMR (600 MHz, $CDCl_3$): δ = 8.76 (s, 4H), 7.57 (d, J = 8 Hz, 1H), 7.49 (d, J = 8 Hz, 1H), 6.85 (d, J = 10 Hz, 1H), 6.79 (d, J = 10 Hz, 1H), 6.63 (d, J = 6 Hz, 1H), 6.55 (d, J = 7 Hz, 1H), 5.24 (m, 2H), 4.86 (m, 2H), 4.59 (m, 2H), 4.46 (m, 2H), 4.15 (t, J = 8 Hz, 2H), 3.59 (s, 3H), 2.82 (s, 3H), 2.81 (s, 3H), 1.9–1.4 (overlapping multiplets), 1.36 (d, J = 7 Hz, 3H), 1.31 (d, J = 7 Hz, 6H), 1.23 (s, 3H), 0.98–0.84 ppm (overlapping doublets, 24H); ESI-TOF MS: found: 1085.6030 $[M+H]^+$; calcd 1085.6030.

Linear precursor to 5: The linear peptide was synthesized from Fmoc-Orn(MTT) Wang polystyrene resin (204 mg, 0.10 mmol) and purified as described above for **12** to yield the trifluoroacetate salt of the product (39 mg, 24%) as a white solid. MALDI-FTMS: found: 1479.7511 $[M+H]^+$; calcd 1479.7558).

Cyclic 5: The linear precursor (39 mg, 24.4 μ mol) was cyclized as described for **4** to yield the product (33 mg, 93%) as an off-white solid. 1H NMR (500 MHz, $CDCl_3$): δ = 8.70 (s, 8H), 7.55 (d, J = 8 Hz, 2H), 6.78 (d, J = 10 Hz, 2H), 6.55 (d, J = 7 Hz, 2H), 5.21 (q, J = 7 Hz, 2H), 4.84 (dd, J = 7, 8 Hz, 2H), 4.72 (dd, J = 6, 6 Hz, 2H), 4.47 (td, J = 10, 4 Hz), 4.19 (m, 4H), 4.04 (d, J = 7 Hz, 4H), 2.81 (s, 6H), 2.2 (m, 2H), 1.98 (m, 2H), 1.85–1.40 (m, 18H), 1.30 (d, J = 7 Hz, 6H), 0.98 (d, J = 7 Hz, 12H), 0.92 ppm (m, 24H); MALDI-FTMS: found: 1483.7228 $[M+Na]^+$; calcd 1483.7272.

Concentration-dependent NMR for *N*-Me cyclic peptides:^[19a] All spectra were obtained in $CDCl_3$ (99.96% from Cambridge Isotope Labs). A stock solution of freshly dried peptide was made in $CDCl_3$, and this solution was sonicated and centrifuged to remove any insoluble material. The concentration of this stock solution was determined by absorption spectroscopy (NDI $\epsilon_{380} = 29850 \text{ cm}^{-1} \text{ M}^{-1}$). The stock solution was then diluted to make samples at the desired concentrations (at least three different concentrations for each peptide). 1H NMR spectra were obtained on a Bruker DRX 500 or DRX 600 spectrometer. As the monomer and dimer species are in slow exchange on the NMR timescale, peaks for both species were visible. The data were fit to the model given in Equations (1) and (2), where $[A]$ and $[A_2]$ are the concentrations of monomer and dimer, respectively, and C_{tot} is the total concentration.

$$K = \frac{[A_2]}{[A]^2} \quad (1)$$

$$C_{\text{tot}} = 2[A_2] + [A] \quad (2)$$

The integrated intensities of the backbone *N*-methyl groups were used to measure the ratio of the two species. A variable x was defined according to Equation (3), where I_{dimer} is the integrated intensity of dimer *N*-methyl peaks and I_{monomer} is the integrated intensity of monomer *N*-methyl peaks.

$$x \equiv \frac{I_{\text{dimer}}}{2I_{\text{monomer}}} = \frac{[A_2]}{[A]} \quad (3)$$

Combining Equations (1)–(3) gives Equation (4).

$$C_{\text{tot}} = \frac{2x^2 + x}{K} \quad (4)$$

The equilibrium constant for dimerization (K) was found from the inverse of the slope of the linear fit of C_{tot} against $(2x^2 + x)$ for each experimental concentration.

Self-association constant of 7 by NMR spectroscopy:^[29] NDI control compound **7** demonstrated concentration-dependent chemical shifts over the 1 to 50 mM range. This concentration-dependent behavior was modeled as a monomer and dimer in equilibrium and in fast exchange on the NMR timescale. The data was modeled in terms of the self-association equilibrium shown in Equations (1) and (2) above. For a given C_{tot} and an arbitrary value of K , $[A]$ can be found from the root of Equation (5), where $[A]$ is greater than 0 and less than C_{tot} .

$$2[A]^2K + [A] - C_{\text{tot}} = 0 \quad (5)$$

If equilibrium between monomer and dimer in fast exchange is assumed, the chemical shift for a given proton in **7** follows Equation (6), where δ is the observed chemical shift, δ_1 is the chemical shift of the monomer, and δ_2 is the chemical shift of the dimer.

$$\delta = \frac{2K[A]^2}{C_{\text{tot}}}(\delta_2 - \delta_1) + \delta_1 \quad (6)$$

Thus, observed δ values for each experimentally determined C_{tot} are used

with an arbitrary K in Equation (7) to determine δ_1 and δ_2 by linear regression analysis. These values are in turn used to calculate a theoretical

$$\frac{2K[A]^2}{C_{\text{tot}}} \quad (7)$$

δ value for each experimental concentration. Numerical minimization of the sum of the squares of the residuals between observed and calculated δ values gave the best fit when $K = 0.44\text{m}^{-1}$.

Fluorescence measurements: Stock solutions were prepared in CDCl_3 as described above for the concentration-dependent NMR experiments. Samples were measured in a 0.2×1 cm quartz cuvette (0.2 cm along excitation path). The excitation wavelength was 330 nm and the detector voltage was kept the same for all samples.

Acknowledgements

We thank the National Institute of Health (GM52190) and the Air Force Office of Scientific Research (F49620-00-1-0283) for financial support. W.S.H. thanks the National Science Foundation for a Predoctoral Fellowship, and N.A. thanks the Fulbright Foundation for a Postdoctoral Fellowship.

- [1] For a review, see: D. T. Bong, T. D. Clark, J. R. Granja, M. R. Ghadiri, *Angew. Chem.* **2001**, *113*, 1016–1041; *Angew. Chem. Int. Ed.* **2001**, *40*, 988–1011.
- [2] Cyclic $\text{D,L-}\alpha$ -peptides: a) M. R. Ghadiri, J. R. Granja, R. A. Milligan, D. E. McRee, N. Khazanovich, *Nature* **1993**, *366*, 324–327; b) J. D. Hartgerink, J. R. Granja, R. A. Milligan, M. R. Ghadiri, *J. Am. Chem. Soc.* **1996**, *118*, 43–50; c) K. Rosenthal-Aizman, G. Svensson, A. Unden, *J. Am. Chem. Soc.* **2004**, *126*, 3372–3373.
- [3] Cyclic β -peptides: a) T. D. Clark, L. K. Buehler, M. R. Ghadiri, *J. Am. Chem. Soc.* **1998**, *120*, 651–656; b) D. Seebach, J. L. Matthews, A. Meden, T. Wessels, C. Baerlocher, L. B. McCusker, *Helv. Chim. Acta* **1997**, *80*, 173–182.
- [4] Cyclic α,β -peptides: I. L. Karle, B. K. Handa, C. H. Hassall, *Acta Crystallogr.* **1975**, *B31*, 555–560.
- [5] Cyclic α,γ -peptides: M. Amorin, L. Castedo, J. R. Granja, *J. Am. Chem. Soc.* **2003**, *125*, 2844–2845.
- [6] Cyclic δ -peptides: D. Gauthier, P. Baillargeon, M. Drouin, Y. L. Dory, *Angew. Chem.* **2001**, *113*, 4771–4774; *Angew. Chem. Int. Ed.* **2001**, *40*, 4635–4638.
- [7] Cyclic oligoureas: a) D. Ranganathan, C. Lakshmi, I. L. Karle, *J. Am. Chem. Soc.* **1999**, *121*, 6103–6107; b) V. Semetey, C. Didierjean, J.-P. Briand, A. Aubry, G. Guichard, *Angew. Chem.* **2002**, *114*, 1975–1978; *Angew. Chem. Int. Ed.* **2002**, *41*, 1895–1898.
- [8] Cyclic α,ϵ -peptides: W. S. Horne, C. D. Stout, M. R. Ghadiri, *J. Am. Chem. Soc.* **2003**, *125*, 9372–9376.
- [9] a) M. R. Ghadiri, J. R. Granja, L. K. Buehler, *Nature* **1994**, *369*, 301–304; b) J. R. Granja, M. R. Ghadiri, *J. Am. Chem. Soc.* **1994**, *116*, 10785–10786; c) J. Sanchez-Quesada, M. P. Isler, M. R. Ghadiri, *J. Am. Chem. Soc.* **2002**, *124*, 10004–10005; d) J. Sanchez-Quesada, H. S. Kim, M. R. Ghadiri, *Angew. Chem.* **2001**, *113*, 2571–2574; *Angew. Chem. Int. Ed.* **2001**, *40*, 2503–2506; e) S. Fernandez-Lopez, H.-S. Kim, E. C. Choi, M. Delgado, J. R. Granja, A. Khasanov, K. Kraehenbuehl, G. Long, D. A. Weinberger, K. M. Wilcoxon, M. R. Ghadiri, *Nature* **2001**, *412*, 452–456.
- [10] a) M. S. Vollmer, T. D. Clark, C. Steinem, M. R. Ghadiri, *Angew. Chem.* **1999**, *111*, 1703–1706; *Angew. Chem. Int. Ed.* **1999**, *38*, 1598–1601; b) C. Steinem, A. Janshoff, M. S. Vollmer, M. R. Ghadiri, *Langmuir* **1999**, *15*, 3956–3964; c) K. Motesharei, M. R. Ghadiri, *J. Am. Chem. Soc.* **1997**, *119*, 11306–11312.
- [11] a) A. Bachtold, P. Hadley, T. Nakanishi, C. Dekker, *Science* **2001**, *294*, 1317–1320; b) C. P. Collier, G. Mattersteig, E. W. Wong, Y. Luo, K. Beverly, J. Sampaio, F. M. Raymo, J. F. Stoddart, J. R. Heath, *Science* **2000**, *289*, 1172–1175; c) Y. Huang, X. Duan, Q. Wei, C. M. Lieber, *Science* **2001**, *291*, 630–633; d) C. Joachim, J. K. Gimzewski, A. Aviram, *Nature* **2000**, *408*, 541–548; e) J. M. Tour, *Acc. Chem. Res.* **2000**, *33*, 791–804.
- [12] a) P. Carloni, W. Andreoni, M. Parrinello, *Phys. Rev. Lett.* **1997**, *79*, 761–764; b) R. A. Jishi, N. C. Braier, C. T. White, J. W. Mintmire, *Phys. Rev. B* **1998**, *58*, R16009–R16011; c) J. P. Lewis, N. H. Pawley, O. F. Sankey, *J. Phys. Chem. B* **1997**, *101*, 10576–10583; d) H. Okamoto, T. Nakanishi, Y. Nagai, M. Kasahara, K. Takeda, *J. Am. Chem. Soc.* **2003**, *125*, 2756–2769; e) H. Okamoto, K. Takeda, K. Shiraishi, *Phys. Rev. B* **2001**, *64*, 115425/1–115425/17.
- [13] a) M. Pope, C. E. Swenberg, *Electronic Processes in Organic Crystals and Polymers*, Oxford Science Publications, Oxford, **1999**; for recent examples see: b) V. Percec, M. Glodde, T. K. Bera, Y. Miura, I. Shiyonovskaya, K. D. Singer, V. S. K. Balagurusamy, P. A. Heiney, I. Schnell, A. Rapp, H.-W. Spiess, S. D. Hudson, H. Duan, *Nature* **2002**, *419*, 384–387; c) L. Schmidt-Mende, A. Fechtenkötter, K. Müllen, E. Moons, R. H. Friend, J. D. MacKenzie, *Science* **2001**, *293*, 1119–1122.
- [14] H. Rapaport, H. S. Kim, K. Kjaer, P. B. Howes, S. Cohen, J. Als-Nielsen, M. R. Ghadiri, L. Leiserowitz, M. Lahav, *J. Am. Chem. Soc.* **1999**, *121*, 1186–1191.
- [15] a) H. E. Katz, J. Johnson, A. J. Lovinger, W. Li, *J. Am. Chem. Soc.* **2000**, *122*, 7787–7792; b) H. E. Katz, A. J. Lovinger, J. Johnson, C. Kloc, T. Slegrist, W. Li, Y.-Y. Lin, A. Dodabalapur, *Nature* **2000**, *404*, 478–481.
- [16] a) L. L. Miller, K. R. Mann, *Acc. Chem. Res.* **1996**, *29*, 417–423; b) L. L. Miller, R. G. Duan, D. C. Tully, D. A. Tomalia, *J. Am. Chem. Soc.* **1997**, *119*, 1005–1010; c) I. Tabakovic, L. L. Miller, R. G. Duan, D. C. Tully, D. A. Tomalia, *Chem. Mater.* **1997**, *9*, 736–745.
- [17] D. T. Bong, M. R. Ghadiri, *Angew. Chem.* **2001**, *113*, 2221–2224; *Angew. Chem. Int. Ed.* **2001**, *40*, 2163–2166.
- [18] $\text{D,L-}\alpha$ -Hexapeptides: M. Saviano, L. Zaccaro, A. Lombardi, C. Pedone, B. Di Blasio, X. Sun, G. P. Lorenzi, *J. Inclusion Phenom.* **1994**, *18*, 27–36.
- [19] $\text{D,L-}\alpha$ -Octapeptides: a) T. D. Clark, J. M. Buriak, K. Kobayashi, M. P. Isler, D. E. McRee, M. R. Ghadiri, *J. Am. Chem. Soc.* **1998**, *120*, 8949–8962; b) M. R. Ghadiri, K. Kobayashi, J. R. Granja, R. K. Chadha, D. E. McRee, *Angew. Chem.* **1995**, *107*, 76–78; *Angew. Chem. Int. Ed. Engl.* **1995**, *34*, 93–95.
- [20] a) T. D. Clark, M. R. Ghadiri, *J. Am. Chem. Soc.* **1995**, *117*, 12364–12365; b) T. D. Clark, K. Kobayashi, M. R. Ghadiri, *Chem. Eur. J.* **1999**, *5*, 782–792; c) K. Kobayashi, J. R. Granja, M. R. Ghadiri, *Angew. Chem.* **1995**, *107*, 79–82; *Angew. Chem. Int. Ed. Engl.* **1995**, *34*, 95–98.
- [21] T. Wagner, W. B. Davis, K. B. Lorenz, M. E. Michel-Beyerle, U. Dieberichsen, *Eur. J. Org. Chem.* **2003**, 3673–3679.
- [22] A. A. Mokhir, R. Kraemer, *Bioconjugate Chem.* **2003**, *14*, 877–883.
- [23] W. J. Sep, J. W. Verhoeven, T. J. De Boer, *Tetrahedron* **1975**, *31*, 1065–1070.
- [24] E. Buncel, N. L. Mailloux, R. S. Brown, P. M. Kazmaier, J. Dust, *Tetrahedron Lett.* **2001**, *42*, 3559–3562.
- [25] E. L. Eliel, S. H. Wilen, L. N. Mander, *Stereochemistry of Organic Compounds*, Wiley, New York, **1994**.
- [26] S. W. Benson, *J. Am. Chem. Soc.* **1958**, *80*, 5151–5154.
- [27] T. C. Barros, S. Brochsztain, V. G. Toscano, P. Berci Filho, M. J. Politi, *J. Photochem. Photobiol. A* **1997**, *111*, 97–104.
- [28] a) S. A. Kates, N. A. Solé, C. R. Johnson, D. Hudson, G. Barany, F. Albericio, *Tetrahedron Lett.* **1993**, *34*, 1549–1552; b) J. E. Redman, K. M. Wilcoxon, M. R. Ghadiri, *J. Comb. Chem.* **2003**, *5*, 33–40.
- [29] K. A. Connors, *Binding Constants: The Measurement of Molecular Complex Stability*, Wiley, New York, **1987**.

Received: September 9, 2004
Published online: December 29, 2004